

DOI: 10.1002/cmdc.201300372

Discovery of Potent HDAC Inhibitors Based on Chlamydocin with Inhibitory Effects on Cell Migration

Shimiao Wang,^[a] Xiaohui Li,^{*[a]} Yingdong Wei,^[a] Zhilong Xiu,^[a] and Norikazu Nishino^[b]

The histone deacetylase (HDAC) family is a promising drug target class owing to the importance of these enzymes in a variety of cellular processes. Docking studies were conducted to identify novel HDAC inhibitors. Subtle modifications in the recognition domain were introduced into a series of chlamydocin analogues, and the resulting scaffolds were combined with various zinc binding domains. Remarkably, *cyclo*(L-Asu(NHOH)-L-A3mc6c-L-Phe-D-Pro, compound **1b**), with a methyl group at positions 3 or 5 on the aliphatic ring, exhibited better antiproliferative effects than trichostatin A (TSA) against MCF-7 and

K562 cell lines. In addition to cell-cycle arrest and apoptosis, cell migration inhibition was observed in cells treated with compound **1b**. Subsequent western blot analysis revealed that the balance between matrix metalloproteinase 2 (MMP2) and tissue inhibitors of metalloproteinase 1 (TIMP1) determines the degree of metalloproteinase activity in MCF-7 cells, thereby regulating cell migration. The improved inhibitory activity imparted by altering the hydrophobic substitution pattern at the bulky cap group is a valuable approach in the development of novel HDAC inhibitors.

Introduction

Posttranslational modifications such as the acetylation and methylation of histones are implicated in various cellular processes, including chromatin remodeling, expression silencing, and DNA repair.^[1,2] Aberrant histone deacetylation has been shown to be associated with tumorigenesis and tumor development. The dynamics of acetylation at histone N-terminal tails (such as H3K4 and H4K16) is mediated by histone acetyltransferases (HATs) and histone deacetylases (HDACs).^[3] Eighteen human HDAC members have been identified so far, and these are divided into four classes based on size, cellular localization, number of catalytic sites, and homology to yeast proteins. Class I (HDACs 1, 2, 3, and 8), class IIa (HDACs 4, 5, 7, and 9), class IIb (HDACs 6 and 10), and class IV (HDAC11) HDACs are all zinc-dependent enzymes, whereas class III HDACs are strictly dependent on NAD⁺ for their activities. Further knock-out analyses of various class I and II HDAC proteins have indicated that class I HDACs play a key role in cell survival and proliferation, and class II HDACs may have tissue-specific functions.^[4]

To date, thousands of non-histone proteins have been identified as HDAC substrates.^[5,6] As HDACs are well-validated anticancer targets, it is well known that HDAC inhibitors mediate cell death via multiple pathways. Cell-cycle arrest, apoptosis, differentiation, and anti-angiogenic effects have been observed

in cells treated with HDAC inhibitors.^[7] Furthermore, HDAC6, a unique HDAC containing two intact catalytic domains, has already been identified as a key regulator of cell migration.^[8] In addition, there is increasing evidence to suggest that HDAC4 plays a significant role in cell migration by regulating the expression of matrix metalloproteinase (MMP) family members.^[9,10]

There are typically three functional domains in the structure of HDAC inhibitors: a zinc binding domain (ZBD, usually a hydroxamate or thiol moiety), a surface recognition domain (SRD, generally an aromatic moiety), and a linker domain (typically an aliphatic chain). Based on the structure of natural and synthetic compounds such as trichostatin A (TSA), vorinostat (suberoylanilide hydroxamic acid, SAHA), chlamydocin, and FK228 (Figure 1), numerous HDAC inhibitors have been developed as potential anticancer agents. There are currently several HDAC inhibitors undergoing clinical trials.^[11,12] Two of them, SAHA and FK228, have already been approved by the US Food and Drug Administration (FDA) for the treatment of cutaneous T-cell lymphoma (CTCL).

In our previous work, a novel chlamydocin–hydroxamic acid analogue, *cyclo*(L-Asu(OBn)-Aib-L-Phe-D-Pro) (Ky-2), was identified as a potential anticancer agent and was shown to induce apoptosis in myeloma cells.^[13] Therefore, docking studies were initially carried out to analyze the binding mode of HDAC inhibitors to HDAC. Consistent with the previous study, the interactions between Ky-2 and HDAC2 further confirmed that the changes brought about in the aminoisobutyric acid (Aib) site or to the aromatic ring of L-Phe would affect HDAC inhibitory activity.^[14,15] In this study, unnatural amino acids 1-amino-*n*-methyl-1-cyclohexanecarboxylic acid (Anmc6c), L-2-amino-chloro-*n*-aliphatic acid (L-Acn), or *n*-chlorophenylalanine (L-Phe(*n*Cl)) were used to substitute the corresponding residues Aib

[a] S. Wang, Dr. X. Li, Y. Wei, Z. Xiu
School of Life Science and Biotechnology
Dalian University of Technology, 2 Linggong Road, 116024 Dalian (China)
E-mail: lxhxh@dlut.edu.cn

[b] Dr. N. Nishino
Graduate School of Life Science and Systems Engineering
Kyushu Institute of Technology, 808-0196 Kitakyushu (Japan)

 Supporting information for this article is available on the WWW under <http://dx.doi.org/10.1002/cmdc.201300372>.

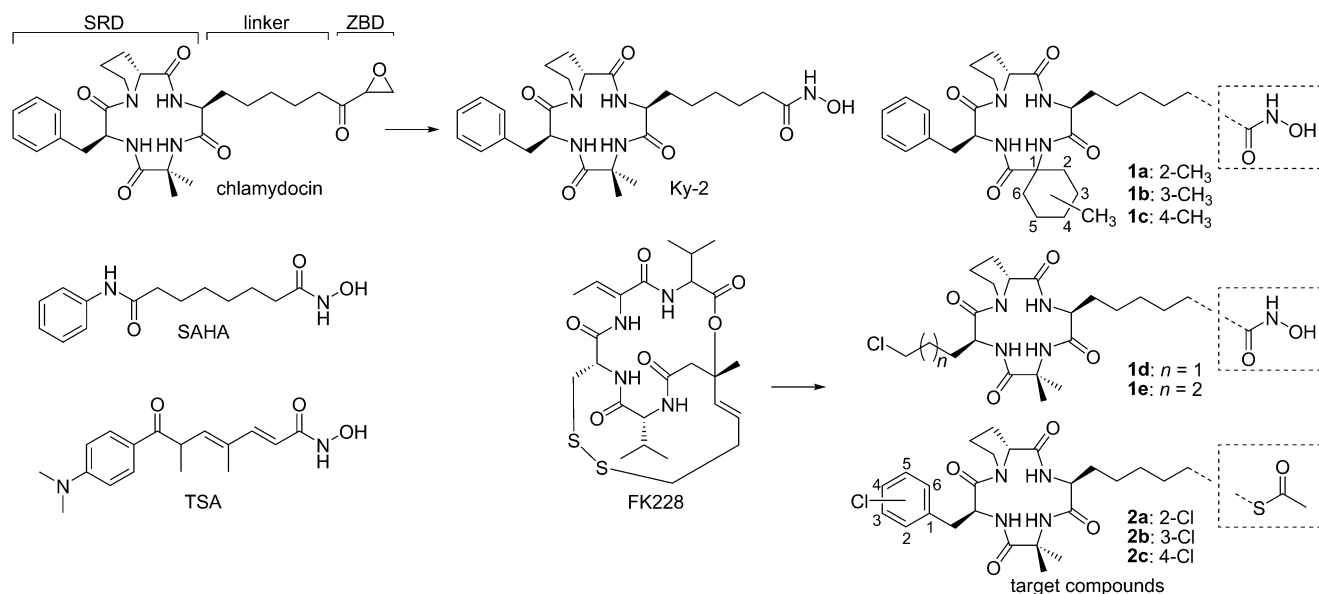


Figure 1. Classic HDAC inhibitors and target compounds.

(marked as AA₂ according to its position in Ky-2) or L-Phe (marked as AA₃), and the resulting scaffolds were combined with either hydroxamate or a thioacetyl group (Figure 1). The inhibitory activities against HDAC isoforms and antiproliferative activities of these compounds were then evaluated. Furthermore, key regulators that mediate cell cycle and cell migration were explored to determine the underlying mechanisms of HDAC-inhibitor-induced cell death.

Results and Discussion

Molecular design

It is well known that HDACs, especially the class I subfamily (HDACs 1, 2, and 3), are generally expressed in nearly all cancer tissue types. HDAC1 and HDAC2 are highly similar, sharing an overall sequence identity of ~82%, suggesting either of them is qualified to represent the class I enzymes.^[16,17] Therefore, to explore the binding mode of the chlamydocin-hydroxamic acid analogue to HDAC, a docking study was performed with the HDAC2–Ky-2 complex. In the docking of Ky-2, the compound binds very well to the active site of HDAC2: the aliphatic chain of Ky-2 occupies the long and narrow channel of HDAC2, the Aib and L-Phe residues from the bulky SRD interact with the residues at the entrance of the active site, while the hydroxamic acid group chelates to the zinc ion at the bottom of the catalytic pocket (Figure 2). In HDAC2–Ky-2 complex, the aromatic ring of the phenyl group is oriented into the groove formed by Tyr209 and Phe210, thus contributing to the stabilization of the enzyme–inhibitor complex.

Hydrogen bonds and hydrophobic contacts between HDAC2 and Ky-2 were then analyzed (Figure 3). In the HDAC2–Ky-2 complex, the oxygen atom from the hydroxamate group of Ky-2 establishes a hydrogen bond with the Nε2 atom of His145, while the nitrogen atom of Ky-2 establishes hydrogen bonds

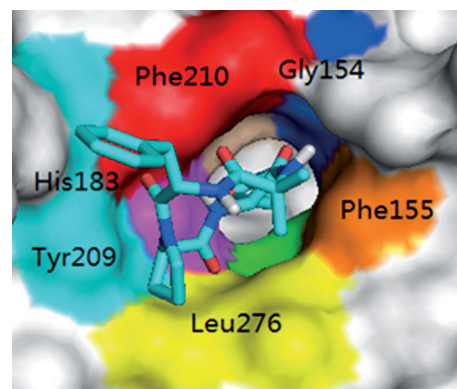


Figure 2. Binding mode of Ky-2 (stick model) in HDAC2 as predicted by docking; HDAC2 residues that interact with Ky-2 are indicated.

with Nε2 of His145, Nε2 of His146, and Oδ2 of Asp181. Because the hydrogen bonds formed between the hydroxylamine group in the metal binding domain and the corresponding residues around the active pocket of HDAC2 were expected to be crucial for HDAC inhibitory activity, the hydroxamate moiety was maintained in the newly designed compounds 1a–e (Figure 1).

Previous studies have demonstrated that thiols are potent zinc binding groups (ZBGs).^[18] Docking studies further revealed that the sulfur atom of the thiol group can effectively interact with His183 and Tyr308 of HDAC2 through hydrogen bonds.^[19] In the meantime, evidence emerged to suggest that thioacetyl derivatives might be as effective as thiol derivatives.^[20] In contrast to disulfides, mass spectrometry revealed that thioacetyl groups remain intact after inhibition.^[20] Therefore, to develop potent non-hydroxamate HDAC inhibitors, a thioacetyl group was introduced into desired compounds 2a–c (Figure 1).

The hydrophobic interactions between Aib and L-Phe residues of Ky-2 and His183, Glu208, Tyr209, Phe210, and Gly306

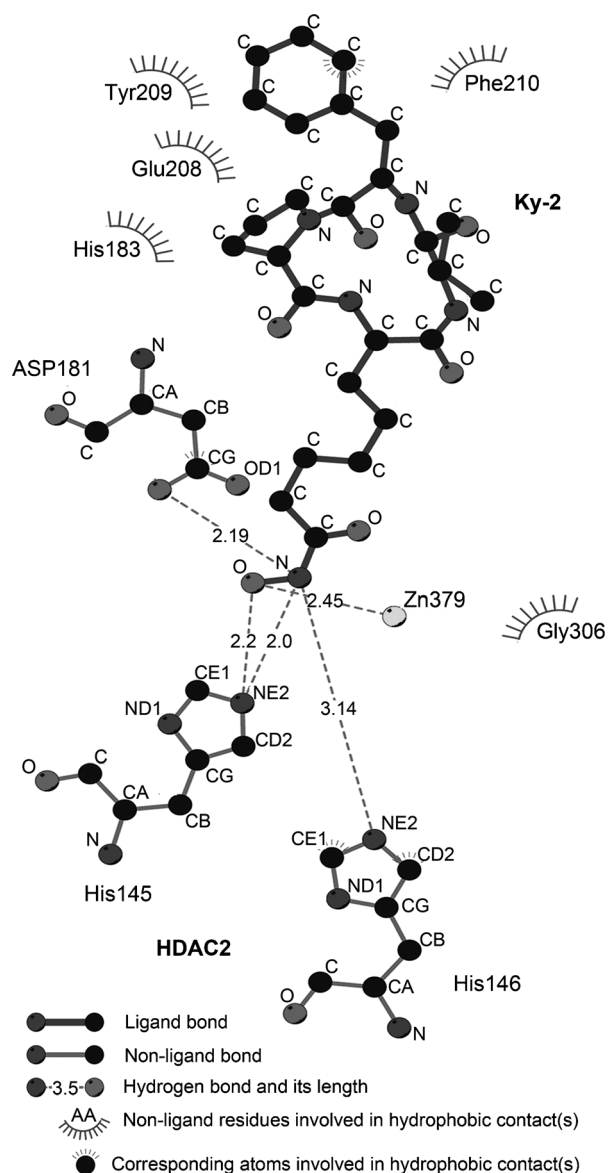


Figure 3. Hydrogen bonds and hydrophobic contacts between HDAC2 and Ky-2. Distances between hydrogen bond donors and acceptors less than 3.5 Å are represented as dashed lines.

residues of HDAC2 are favorable to the stabilization of the enzyme–inhibitor complex (Figure 3). These findings suggest that further modification of the SRD to affect hydrophobic properties may ultimately alter HDAC inhibitory activity.^[21] Therefore, an aliphatic ring, aliphatic chain, or further modifications to the aromatic ring of L-Phe were introduced into our desired compounds to alter surface hydrophobicity. Specifically, Anmc6c was used to replace Aib to obtain compounds **1a–c**, L-Acn was used to substitute L-Phe for compounds **1d,e**, and L-Phe(*n*Cl) groups were used to replace L-Phe to obtain compounds **2a–c** (Figure 1).

To determine whether all the designed compounds can bind to the active pocket of HDACs and thus have HDAC inhibitory activity, docking studies were conducted before their synthesis. Similar to Ky-2, all target compounds were successfully docked

into the active pocket of HDAC2 (Supporting Information figure S1). All target compound–HDAC2 complexes were predicted to be stable, as their binding energies were similar to that of the reference compound Ky-2 (Supporting Information table S1). In particular, compounds **1a–c** and **2b,c** showed significantly higher HDAC2 binding potential than Ky-2, and therefore were expected to have improved inhibitory activity over Ky-2.

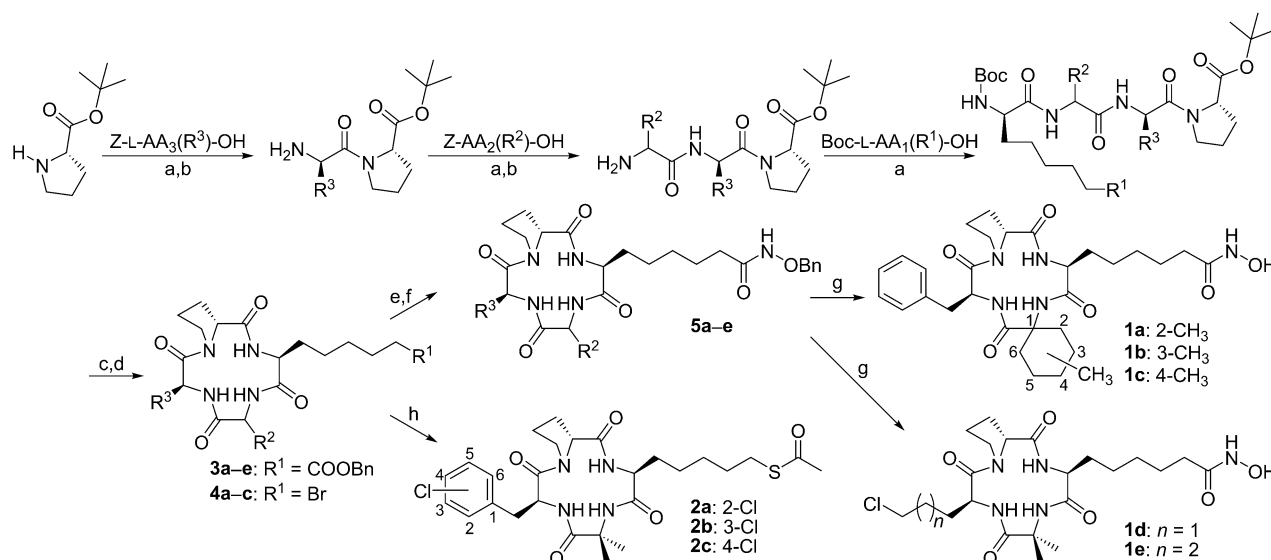
Chemistry

All target compounds were prepared by solution-phase peptide synthesis as illustrated in Scheme 1. Briefly, C-terminal-protected proline (NH₂-D-Pro(OtBu)) was coupled with Z-L-AA₃-OH to give the dipeptide Z-L-AA₃-D-Pro(OtBu). After removal of the Z protecting group via catalytic hydrogenation, the same coupling procedure was used to obtain the tripeptide Z-AA₂-L-AA₃-D-Pro(OtBu) and the tetrapeptide Boc-L-AA₁-AA₂-L-AA₃-D-Pro(OtBu). The corresponding N-terminal (Boc) and C-terminal (OtBu) protecting groups of the linear tetrapeptide were subsequently removed in the presence of trifluoroacetic acid (TFA), and then cyclized in *N,N*-dimethylformamide (DMF) using *O*-(7-azabenzotriazol-1-yl)-1,1,3,3-tetramethyluronium hexafluorophosphate (HATU) and *N,N*-diisopropylethylamine (DIEA) as coupling reagents to give *cyclo*(L-AA₁-AA₂-L-AA₃-D-Pro(OtBu)).

To obtain the hydroxamic acid derivatives, the OBn protecting group of **3a–e** was removed by catalytic hydrogenation, and the hydrogenated residues were subsequently treated with hydroxylamine hydrochloride (HCl·NH₂OBn) in DMF to give **5a–e**. The OBn-protected hydrochlorides **5a–e** were finally transformed by catalytic hydrogenation into the target compounds **1a–e**. For the preparation of non-hydroxamate ZBD, potassium thioacetate was added to **4a–c** with stirring to give the desired thioacetyl derivatives **2a–c**. All target compounds were characterized by ¹H NMR and HR-FAB-MS. The purity of the final products was confirmed by HPLC analysis, and all compounds showed purity > 97%.

Inhibitory activity against HDAC isoforms

The inhibitory activities of all target compounds against class I HDAC1, class IIa HDAC4, and class IIb HDAC6 were measured by using whole-cell extracts prepared from transfected 293T cells. TSA and Ky-2 were used as positive controls. In general, all target compounds exhibited potent HDAC1 inhibitory activities, with IC₅₀ values in the nanomolar range (Table 1). Hydroxamic acid derivatives **1a–e** showed better HDAC inhibitory activities than those of the thioacetyl derivatives **2a–c**. Compared with TSA and Ky-2, the hydroxamic acid derivatives **1a–e** showed increased inhibitory activities against HDACs 1 and 4. Although their HDAC inhibitory activities varied among HDACs 1, 4, and 6, compounds **1a–e** displayed pan-inhibitory activity similar to SAHA and TSA against class I and II HDACs.^[7,22] In particular, compound **1a**, with respective IC₅₀ values of 10 and 6.4 nM against HDACs 1 and 4, showed



Scheme 1. Synthesis of target compounds. *Reagents and conditions:* a) HOBt/DCC in DMF, RT, overnight; b) Pd/C, H₂ in AcOH, RT, overnight; c) TFA, 0 °C, 2 h; d) HATU/DIEA in DMF, RT, 1.5 h; e) Pd/C, H₂ in MeOH, RT, overnight; f) HCl-NH₂OBn, DCC/HOBt in DMF, 0 °C, 2 h; g) Pd/BaSO₄, H₂, RT, overnight; h) KSCoCH₃ in DMF, RT, 4 h.

Table 1. HDAC inhibitory, p21 promoter, and antiproliferative activities of target compounds.

Compd	IC ₅₀ [nM]			p21 EC ₁₀₀₀ [nM] ^[a]		Antiprolif. IC ₅₀ [nM] ^[b]		
	HDAC1	HDAC4	HDAC6	MCF-7	HeLa	K562	HeLa	K562
TSA	23	34	65	20.0 ± 2.7	141 ± 4	39 ± 7	560 ± 55	
Ky-2	18	17	230	18.0 ± 0.54	ND ^[c]	ND	ND	
1a	10	6	130	8.0 ± 0.29	31 ± 3	309 ± 6	876 ± 182	
1b	15	14	160	2.9 ± 0.93	26 ± 1	48 ± 1	104 ± 14	
1c	11	12	170	4.3 ± 1.5	42 ± 4	232 ± 7	863 ± 87	
1d	14	19	110	210.0 ± 48	> 1000	ND	ND	
1e	10	15	96	36.0 ± 2.6	> 1000	ND	ND	
2a	27	ND	> 1000	ND	> 1000	> 1000	> 5000	
2b	28	ND	380	ND	> 1000	480 ± 10	> 5000	
2c	38	ND	> 1000	ND	820 ± 27	630 ± 12	> 5000	

[a] Compound concentration at which the induced luciferase activity is 10-fold higher than the basal level.
[b] Cells were treated for 48 h. [c] ND: no data. All data represent the mean ± SD of at least three independent experiments.

a three- to fivefold increase in enzyme inhibitory activity relative to reference compounds, respectively.

The hydroxamic acid derivatives with variations at the aliphatic ring (compounds **1a–c**) showed no significant differences in HDAC1, 4, and 6 inhibitory activities. Likewise, the thioacetyl derivatives bearing variations at the aromatic ring (**2a–c**) showed similar activity in HDAC1 inhibitory activities. Dramatic differences were observed, however, among the thioacetyl derivatives **2a–c** in HDAC6 inhibitory activities. Compound **2b**, bearing a *meta*-chlorine on the aromatic ring, exhibited higher HDAC6 inhibitory activity than the other two, suggesting modifications at the *meta* position as suitable for improving inhibitory activity. Substitution of the chlorine atom on the aromatic ring for phenyl or furyl groups is expected to produce even more potent HDAC6-selective inhibitors.^[23,24]

All tested compounds showed selectivity for HDAC1 over HDAC6. Although compounds **1a–e** displayed lower inhibitory

activity against HDAC6 than TSA, their IC₅₀ values toward HDAC6 were slightly higher than that of Ky-2. The unique tandem-arranged catalytic pockets of HDAC6 provide an explanation for the observed selectivity, suggesting that small molecules such as TSA might be more favorable to the HDAC6-inhibitor interaction.^[25,26] Furthermore, the aliphatic ring from hydroxamic acid derivatives **1a–c** and the aliphatic ring from **1d,e** are more hydrophobic than the corresponding moieties in the precursor compound Ky-2 (Supporting

Information table S1), thus leading to better HDAC6 inhibitory activity.

p21 promoter activation

All the hydroxamic acid derivatives **1a–e** including reference compounds TSA and Ky-2 were tested for their ability to activate the p21 promoter. All tested compounds effectively activated p21 gene expression, with EC₁₀₀₀ values in the nanomolar range (Table 1). The p21 promoter activation efficiency is ranked in the order: **1b** > **1c** > **1a** > Ky-2 > TSA > **1e** > **1d**. Notably, compound **1b** exhibited the highest activation efficiency, giving an EC₁₀₀₀ value of 2.9 nM, which is at least sixfold lower than that of TSA and Ky-2. Relative to their HDAC inhibitory activities, compounds **1d,e** showed unexpectedly low activation efficiency, which is presumably due to an excess in tor-

sional energy that must be provided to stabilize HDAC-1 d/1 e complex (Supporting Information table S1).

Antiproliferative activity against cancer cell lines

Based on HDAC inhibitory activity and p21 promoter activation efficiency, MTT assays were performed for the hydroxamic acid derivatives **1a–c** and the thioacetyl derivatives **2a–c** to determine their antiproliferative activities against human breast cancer (MCF-7), human cervical cancer (HeLa), and human leukemia cancer (K562) cell lines. TSA was used as a reference compound.

In general, the hydroxamic acid derivatives **1a–c** displayed better antiproliferative activities than the thioacetyl compounds **2a–c**. Similar to their HDAC isoform inhibitory activities, compounds **1a–c** exhibited increased antiproliferative activity over TSA, with their IC_{50} values in the nanomolar range (Table 1). In contrast, the thioacetyl derivatives **2a–c** showed moderate antiproliferative activities, with their IC_{50} values barely in the micromolar range. Among these three cell lines, the antiproliferative activities of **2a–c** were clearly lower against K562. In consideration of the critical function of HDAC6 in HDAC inhibitor-induced leukemia cell death,^[27] the unexpectedly low activities are probably due to their poor HDAC6 inhibitory activity. In addition, aberrant epigenetic modifications on the p21 promoter in leukemia cells may also be responsible for their poor inhibitory activities against the K562 line.^[28] Consistent with their enzyme inhibitory activities, no drastic differences were observed among compounds **2a–c**, suggesting that the position of chlorine on the phenyl ring does not have a significant effect on cellular potency.

The antiproliferative activities of compounds **1a–c** is in the order: MCF-7 > HeLa > K562. In particular, the most active compound, **1b**, gave an IC_{50} value of 26 nM, which is at least fivefold lower than that of TSA (140 nM) against MCF-7 cells. Relative to **1a** and **1c**, attachment of the methyl group at positions 3 or 5 of the aliphatic ring led to increased antiproliferative activity. These results further support this position of the aliphatic ring as a preferred modification site for the design of more potent HDAC inhibitors. Given the clear advantage in cellular potency observed in this assay, compound **1b** was selected for subsequent biological evaluation.

Cell-cycle arrest induced by compound 1b

It has been widely accepted that the inhibition of HDACs leads to cell-cycle arrest in various human cancer cell lines. Cyclin D₁ and p21 are both key regulators of cell proliferation. By binding with cyclin-dependent kinase (CDK), the cyclin D₁-CDK complex promotes cell-cycle progression, whereas p21 blocks cell-cycle progression by inhibiting the activity of the cyclin D₁-CDK complex.^[29,30] Accordingly, cell-cycle distribution and the expression level of relevant regulators p21 and cyclin D₁ in MCF-7 cells were analyzed.

After incubation with compound **1b**, cell-cycle phase distribution dramatically changed, appearing in a concentration-dependent manner (Figure 4a). After incubation for 24 h, the per-

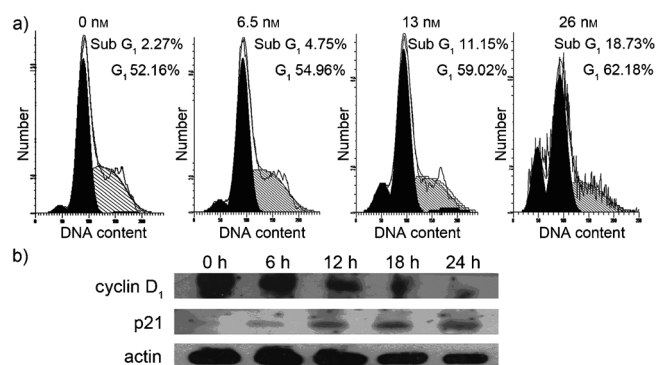


Figure 4. Effects of compound **1b** on cell-cycle arrest in MCF-7 cells. a) MCF-7 cells were treated with indicated the concentrations of **1b** for 24 h, then stained with PI to determine cell-phase distribution. b) Cells were treated with 26 nM **1b** for the indicated times, then analyzed by western blot; β -actin (actin) was used as internal control.

centage of cells in G₀/G₁ phase gradually increased from 52.16 to 62.18%, while that of the sub-G₁ phase increased from 2.27 to 18.73%. During treatment, the expression of cyclin D₁ was decreased rapidly in the first 12 h, whereas the expression of p21 was gradually increased under the same conditions, both appearing in a time-dependent manner (Figure 4b). These results indicate that compound **1b** induces cell-cycle arrest in MCF-7 cells by simultaneously up-regulating the expression of p21 while down-regulating the expression of cyclin D₁.

Furthermore, p21 and cyclin D₁ act as cell-cycle checkpoints that are fatal for cell survival: on the one hand, cell-cycle checkpoints enhance cell survival after DNA damage; on the other hand, programmed cell death pathways like apoptosis might be triggered during DNA repair.^[31] In this study, evidence for a 16% increase in apoptotic peak (sub-G₁ phase) was observed in cells treated with compound **1b**. As apoptosis could be triggered and affected through multiple pathways, further studies are still in progress in our laboratories.

Inhibition of cell migration

Tumor growth and metastasis require a coordinated series of events including degradation of the extracellular matrix, cellular adhesion, migration, and invasion.^[32] Here we used a soft agar assay, which is regarded as an effective substitute for in vivo trials,^[33] to investigate the effect of compound **1b** on cell migration. As shown in Figure 5a, the number of cell colonies significantly diminished after treatment with compound **1b**. After incubation with compound **1b** at 13 nM for 24 h, no colonies were observed. As shown in the enlarged images (Figure 5b), cell masses formed from untreated MCF-7 cells were observed, whereas only a single cell or cell debris were observed after exposure to compound **1b**.

Colony-forming capacity, which is implicated in cancer development and often initiates following cell migration, is speculated to be influenced by the migratory activity of cancer cells.^[34,35] Accordingly, the effect of compound **1b** on colony formation was subsequently examined. Similar to the results observed in the soft agar assay, the number of MCF-7 colonies

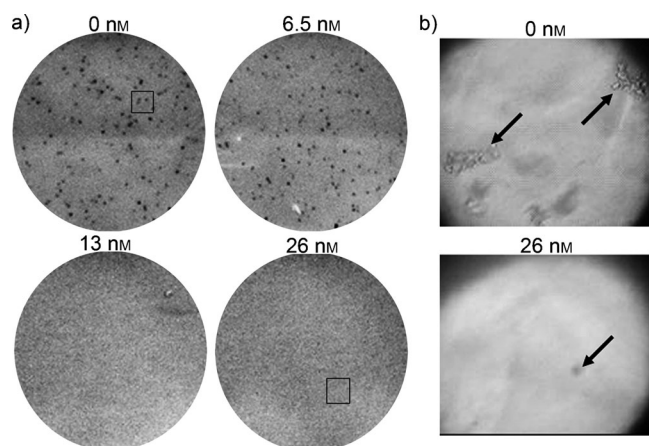


Figure 5. Effects of compound **1b** on cell migration. MCF-7 cells were successively cultured in soft agar for 14 days until the resulting colonies were large enough to be visualized. a) Cells were stained with MTT for colony visualization; each spot represents a single colony. b) Enlarged view of a single cell colony (square fields indicated in panel a).

gradually decreased following prolonged treatment time (Supporting Information figure S2). Nearly 40% of total cell colonies vanished after treatment for 24 h.

Regulating the balance between MMP2 and TIMP1 to inhibit cell migration

MMPs comprise a family of proteases that are capable of degrading the extracellular matrix (ECM). MMP2, a major MMP family member, is secreted as latent enzyme (pro-type, 72 kDa). After cleavage, the obtained active form of MMP2 (66 kDa) is able to modulate cell-matrix interaction, thus modulating cell migration.^[36] To determine the role of MMP2 in compound-**1b**-induced cell migration inhibition, the activity of MMP2 was measured using gelatin zymography. As shown in Figure 6a, the catalytic activity of MMP2 dramatically increased during the first 6 h of treatment. However, the activity of

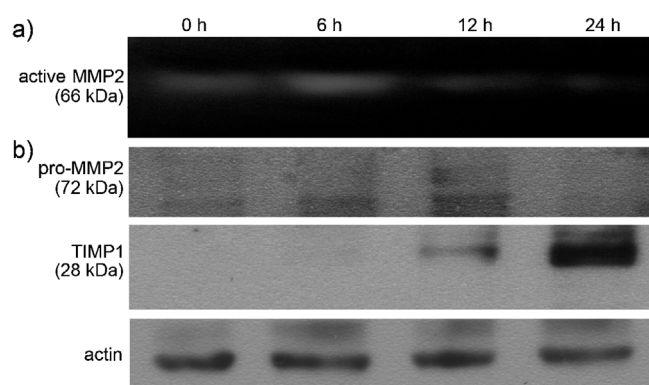


Figure 6. Effects of compound **1b** on regulating the balance between MMP2 and TIMP1. MCF-7 cells were treated with 26 nM **1b** for the times indicated. a) The extracellular activity of MMP2 is gauged as the intensity of transparent bands against a dark background. b) The intracellular expression levels of MMP2 and TIMP1 are presented as dark bands against a grey background. β -actin (actin) was used as internal control.

MMP2 was subsequently decreased if cells were successively treated for more than 12 h. After 24 h treatment with compound **1b**, the activity of MMP2 was barely detectable, suggesting cell migration was inhibited.

TIMP1 is known as a key regulator in the cleavage of pro-MMP2 to its active form. It is believed that the balance between MMP and TIMP determines the actual metalloproteinase activities and controls ECM degradation.^[32] To understand the mechanism underlying the effect of compound **1b** on cell migration inhibition, the expression levels of MMP2 and TIMP1 were then measured. Consistent with the activity variation of MMP2 during treatment, the expression level of MMP2 was slightly increased in cells treated with compound **1b** during the first 12 h (Figure 6b). However, if cells were successively treated for another 12 h, the expression level of MMP2 was dramatically reduced. In contrast, the expression level of TIMP1 was generally increased during the corresponding treatment period. These data indicate that compound **1b** simultaneously regulates the expression levels of MMP2 and TIMP1, thereby disrupting the balance between MMP2 and TIMP1 and leading to cell migration inhibition.

Binding mode of **1b** in HDAC4

It has been speculated that class II HDACs, especially HDAC4 and HDAC6, are associated with cell migration.^[9] The expression profile revealed that HDAC4 expression is up-regulated in breast cancer, whereas HDAC6 expression might be associated with improved survival.^[37,38] Therefore, a docking study was conducted for the HDAC4-**1b** complex, and the hydrogen bonds and hydrophobic contacts between HDAC4 and **1b** were then analyzed (Figure 7).

Compound **1b** binds very well to the active site of HDAC4, exhibiting a binding mode similar to that of the HDAC2-Ky-2 complex. Specifically, in the HDAC4-**1b** complex, the oxygen atom from the hydroxamate group of **1b** establishes a hydrogen bond with the N ϵ 2 atom of His159 and the OH atom of Tyr332, while the nitrogen atom of **1b** establishes hydrogen bonds with N ϵ 2 of His159. Hydrophobic interactions provided by residues such as Asp115, Phe227, Leu299, and Pro298 around the active site of HDAC4 contribute to stabilizing the HDAC4-**1b** complex. In summary, these results are in line with the observed HDAC inhibitory activity of **1b** and provide structural explanations for the clear lack of selectivity of **1b** for HDAC1 over HDAC4.

Conclusions

The binding energy and hydrophobic interactions in the HDAC2-Ky-2 complex predicted by docking studies provides a structural basis for the design of novel HDAC inhibitors. By the introduction of subtle modifications to the SRD, novel cyclic tetrapeptide-based HDAC inhibitors bearing either hydroxamate (**1a-e**) or thioacetyl moieties (**2a-c**) as their ZBG were developed. Chlamydocin-hydroxamic acid analogues **1a-e**, containing either Anmc6c or L-Acn in their framework, exhibited impressive HDAC inhibitory potential over TSA and Ky-

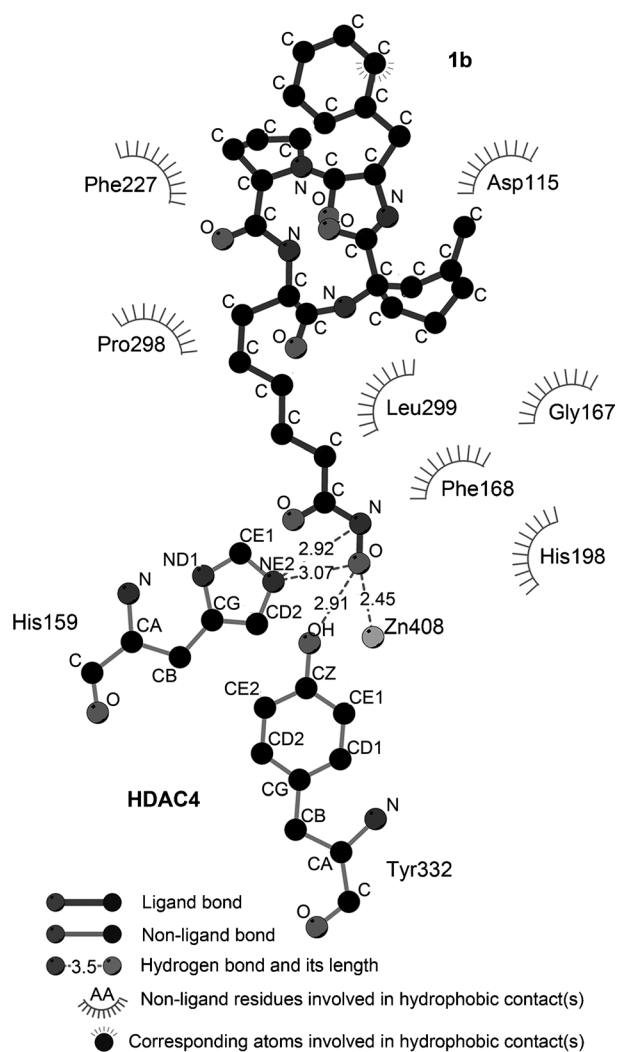


Figure 7. Hydrogen bonds and hydrophobic contacts between HDAC4 and **1b**. Distances between hydrogen bond donors and acceptors less than 3.5 Å are represented as dashed lines.

2. Among them, compound **1b** exhibited the highest antiproliferative activity, with an IC_{50} value of 26 nM against MCF-7 cells. Similar to TSA and Ky-2, cell-cycle arrest and apoptosis were both observed in MCF-7 cells treated with compound **1b**. Furthermore, compound **1b** could effectively inhibit the activity of MMP2, thereby inhibiting cell migration. Western blot analysis further confirmed that **1b**-induced migration inhibition is regulated by interrupting the balance between MMP2 and TIMP1, which is in agreement with previous studies.^[39,40] Recent studies further revealed that HDAC4 silencing would increase the synergistic anticancer activity of combination treatments involving an HDAC inhibitor and cisplatin.^[41] As an effective inhibitor of HDAC1 and HDAC4, compound **1b** could find use as a promising tool for investigating the corresponding molecular mechanisms underlying migration inhibition and combination treatments.

Experimental Section

Materials and measurements

Unless otherwise noted, all solvents and reagents were reagent grade and used without purification. All compounds obtained in each reaction were routinely checked by thin-layer chromatography (TLC) and HPLC. Analytical HPLC was performed on a Hitachi instrument (Japan) equipped with a Chromolith Performance RP-18e column (4.6 × 100 mm, Merck). The mobile phases used were: A: H₂O and 0.1% TFA, B: CH₃CN with 0.1% TFA using a solvent gradient conditions changing linearly from 0% B to 100% B over 15 min at a flow rate of 2 mL min⁻¹; elution was detected by UV absorbance at λ 220 nm. TLC detection was performed on aluminum-backed silica gel plates (Merck DC Alufolien Kieselgel 60 F₂₅₄, Germany) with spots visualized under UV light and after heating. Flash chromatography was performed with silica gel 60 (230–400 mesh) with eluting solvents as indicated. High-resolution fast-atom bombardment mass spectrometry (HR-FAB-MS) data were collected on a JEOL JMS-SX 102A instrument. NMR spectra were recorded on a Varian INOVA 400 MHz spectrometer. All NMR spectra were measured in CDCl₃ with reference to TMS. All ¹H NMR shifts are given in ppm (s = singlet, d = doublet, t = triplet, m = multiplet).

General procedure for the preparation of target compounds 1a–e

All compounds were synthesized according to conventional solution-phase methods;^[14] dicyclohexylcarbodiimide (DCC) and *N*-hydroxybenzotriazole (HOBT) were used as coupling reagents throughout the synthesis. *O*-(7-Azabenzotriazol-1-yl)-1,1,3,3-tetramethyluronium hexafluorophosphate (HATU) was used as cyclization reagent.

cyclo(L-Asu(NHOH)-(±)A2mc6c-L-Phe-D-Pro) (1a): This compound was synthesized according to conventional solution-phase methods. DCC (5 mmol) and HOBT (5.0 mmol) were added to a solution of H-D-Pro(OtBu) (5 mmol) and Z-L-Phe-OH (5 mmol) in DMF (10 mL), and the mixture was stirred overnight to give the dipeptide Z-L-Phe-D-Pro(OtBu). After evaporation of DMF, the Z-protected dipeptide was dissolved in EtOAc and washed with citric acid (10%), NaHCO₃ (4%) and brine. After evaporation of EtOAc, the residue was purified by silica gel chromatography (CHCl₃/MeOH 99:1). The Z-protected dipeptide was subsequently dissolved in AcOH (5 mL), Pd/C (150 mg) was added, and the mixture was stirred under H₂ pressure (150 kPa) overnight to remove the Z group. After filtration and evaporation of AcOH, the N-terminal freed dipeptide was then dissolved in EtOAc and washed with NaHCO₃ (4%). After evaporation of EtOAc, the obtained H-L-Phe-D-Pro(OtBu) was then coupled with Z-(±)A2mc6c-OH using HOBT/DCC in the same manner as described earlier. Tripeptide Z-(±)A2mc6c-L-Phe-D-Pro(OtBu) was deprotected by catalytic hydrogenation to remove the Z group and purified as described earlier to give H-(±)A2mc6c-D-Phe-D-Pro(OtBu). To the N-terminal freed tripeptide, Boc-protected aminosuberic acid benzyl ester (Boc-L-Asu(OBn)) and HOBT/DCC were added to give linear tetrapeptide Boc-L-Asu(OBn)-(±)A2mc6c-L-Phe-D-Pro(OtBu). Boc-protected tetrapeptide was dissolved in TFA (3 mL) at 0 °C and kept for 2 h. The obtained TFA salt was then dissolved in DMF (250 mL), DIEA (1.7 mmol), and highly diluted HATU (0.65 mmol in 100 mL DMF) was added in five separate portions every 30 min as cyclization reagents to give cyclo(L-Asu(OBn)-(±)A2mc6c-L-Phe-D-Pro) in 70% yield. After evaporation of DMF, cyclo(L-Asu(OBn)-(±)A2mc6c-L-Phe-D-Pro) was washed with citric acid, NaHCO₃, and brine as men-

tioned above. The OBn-protected cyclic tetrapeptide was dissolved in MeOH (5 mL), and Pd/C (150 mg) was added to remove the OBn group. The mixture was stirred overnight under H₂ pressure (150 kPa). After filtration and evaporation of MeOH, *cyclo*(L-Asu(±)A2mc6c-L-Phe-D-Pro) was obtained. The cyclic tetrapeptide was then dissolved in DMF, and HCl-NH₂OBn (1.5 mmol) and HOBt/DCC (0.4 mmol) were added to give *cyclo*(L-Asu(NH-OBn)(±)A2mc6c-L-Phe-D-Pro). The OBn group was removed under H₂ pressure with Pd/BaSO₄ as catalyst in the presence of AcOH to yield the desired cyclic tetrapeptide *cyclo*(L-Asu(NHOH)(±)A2mc6c-L-Phe-D-Pro). After filtration, the cyclic tetrapeptide was then purified by gel chromatography and lyophilization. Compound **1a** was obtained as a white powder (328 mg, 11%); *t*_R: 7.36 min (HPLC); mp: 93.4–93.8 °C; ¹H NMR (400 MHz, CDCl₃): δ = 0.78 (d, *J* = 7.2 Hz, 3H), 1.05 (d, *J* = 6 Hz, 1H), 1.24–1.40 (m, 8H), 1.60–1.86 (m, 9H), 2.04 (s, 1H), 2.14 (s, 2H), 2.29 (d, *J* = 7.2 Hz, 1H), 3.19 (m, 1H), 3.24 (m, 1H), 3.47 (s, 1H), 3.50 (m, 1H), 3.84 (m, 1H), 3.98 (m, 1H), 4.32 (m, 1H), 4.73 (m, 1H), 5.20 (t, *J* = 9.2, 8.0 Hz, 1H), 6.41 (s, 1H), 6.46 (s, 1H), 7.18 (d, *J* = 7.2 Hz, 1H), 7.20–7.28 (m, 5H), 7.53 ppm (d, *J* = 10, 1H); ¹³C NMR (100 MHz, CDCl₃): δ = 14.21, 18.68, 21.05, 24.57, 24.86, 25.07, 25.13, 27.28, 27.41, 28.77, 29.32, 32.76, 36.07, 46.98, 52.88, 53.22, 54.91, 57.97, 65.04, 65.83, 125.85, 128.74, 128.74, 129.23, 129.26, 137.09, 171.36, 173.26, 175.22, 175.86 ppm; HRMS: *m/z* [M + H]⁺ calcd for C₃₀H₄₃N₅O₆: 570.3292, found: 570.3306.

cyclo(L-Asu(NHOH)-L-A3mc6c-L-Phe-D-Pro) (**1b**): This compound was synthesized according to *cyclo*(L-Asu(NHOH)(±)A2mc6c-L-Phe-D-Pro) (**1a**) using Z-L-A3mc6c-OH instead of Z-(±)A2mc6c-OH. Compound **1b** was obtained as a white powder (430 mg, 15%); *t*_R: 7.80 min (HPLC); mp: 106.8–107.5 °C; ¹H NMR (400 MHz, CDCl₃): δ = 0.88 (dd, *J* = 4.0, 6.0 Hz, 4H), 1.16 (m, 3H), 1.19–1.30 (m, 6H), 1.48–1.72 (m, 10H), 2.04 (s, 1H), 2.13 (m, 2H), 2.30 (d, *J* = 8.4 Hz, 1H), 2.95 (m, 1H), 3.21 (m, 1H), 3.47 (m, 1H), 3.98 (m, 1H), 4.18 (m, 1H), 4.68 (t, *J* = 6.0 Hz, 1H), 5.12 (m, 1H), 6.38 (s, 1H), 6.46 (s, 1H), 7.18 (d, *J* = 9.2 Hz, 1H), 7.21–7.32 (m, 5H), 7.49 ppm (d, *J* = 10 Hz, 1H); ¹³C NMR (100 MHz, CDCl₃): δ = 22.50, 24.78, 24.99, 25.15, 28.16, 29.04, 29.41, 29.60, 32.69, 33.17, 34.11, 36.07, 41.56, 42.83, 47.11, 53.22, 54.57, 57.85, 62.48, 62.63, 126.94, 128.72, 128.78, 129.25, 129.32, 137.09, 171.22, 172.48, 173.33, 174.36 ppm; HRMS: *m/z* [M + H]⁺ calcd for C₃₀H₄₃N₅O₆: 570.3292, found: 570.3257.

cyclo(L-Asu(NHOH)-A4mc6c-L-Phe-D-Pro) (**1c**): This compound was synthesized according to **1a** using Z-L-A4mc6c-OH instead of Z-(±)A2mc6c-OH. Compound **1c** was obtained as a white powder (398 mg, 14%); *t*_R: 7.60 min (HPLC); mp: 73.5–74.1 °C; ¹H NMR (400 MHz, CDCl₃): δ = 0.77 (d, *J* = 12 Hz, 1H), 0.84 (d, *J* = 5.6 Hz, 3H), 1.25–1.30 (m, 12H), 1.61–1.74 (m, 6H), 2.05 (s, 1H), 2.13–2.29 (m, 4H), 2.94 (d, *J* = 5.2 Hz, 1H), 2.97 (d, *J* = 5.6 Hz, 1H), 3.29 (m, 1H), 3.97 (m, 1H), 4.23 (m, 1H), 4.68 (t, *J* = 6.0 Hz, 1H), 5.15 (dd, *J* = 9.2, 6.4 Hz, 1H), 6.46 (s, 1H), 6.67 (s, 1H), 7.19 (d, *J* = 6.8 Hz, 1H), 7.21–7.28 (m, 5H), 7.53 ppm (d, *J* = 10 Hz, 1H); ¹³C NMR (100 MHz, CDCl₃): δ = 21.63, 24.77, 24.94, 25.05, 25.26, 28.39, 28.70, 29.18, 31.25, 32.56, 32.75, 34.04, 36.26, 35.78, 36.04, 47.03, 53.16, 54.70, 57.82, 61.95, 126.89, 128.71, 128.71, 129.22, 129.22, 137.08, 173.21, 174.31, 174.39, 174.48 ppm; HRMS: *m/z* [M + H]⁺ calcd for C₃₀H₄₃N₅O₆: 570.3292, found: 570.3262.

cyclo(L-Asu(NHOH)-Aib-L-Ac5-D-Pro) (**1d**): This compound was synthesized according to **1a** using Z-Aib-OH instead of Z-(±)A2mc6c-OH, and Z-L-Ac5-OH instead of Z-L-Phe-OH. Compound **1d** was obtained as a white powder (176 mg, 7%); *t*_R: 4.95 min (HPLC); mp: 79.0–79.3 °C; ¹H NMR (400 MHz, CDCl₃): δ = 1.20 (t, 2H), 1.24 (t, 2H), 1.36 (s, 3H), 1.62–1.67 (m, 1H), 1.77 (s, 3H), 1.80–1.96 (m, 2H), 2.15 (m, 1H), 2.88 (s, 1H), 2.95 (s, 1H), 3.55 (m, 3H), 3.72 (m, 1H), 4.26 (ddd, *J* = 7.1, 10.3, 3.3 Hz, 1H), 4.78 (t, *J* = 7.9 Hz,

1H), 4.88 (ddd, *J* = 7.5, 10, 2.9 Hz, 1H), 6.48 (s, 1H), 7.16 (d, *J* = 10 Hz, 1H), 7.45 ppm (d, *J* = 10 Hz, 1H); HRMS: *m/z* [M + H]⁺ calcd for C₂₂H₃₆ClN₅O₆: 502.2433, found: 502.2417. CD spectra can be found in Supporting Information figure S3.

cyclo(L-Asu(NHOH)-Aib-L-Ac6-D-Pro) (**1e**): This compound was synthesized according to **1d** using Z-L-Ac6-OH instead of Z-L-Phe-OH. Compound **1e** was obtained as a white powder (206 mg, 8%); *t*_R: 5.24 min (HPLC); mp: 76.2–77.1 °C; ¹H NMR (400 MHz, CDCl₃): δ = 1.24 (t, 2H), 1.36 (s, 3H), 1.43 (d, *J* = 6.7 Hz, 1H), 1.47 (d, *J* = 6.7 Hz, 1H), 1.49 (t, 2H), 1.16–1.74 (m, 6H), 1.76 (s, 3H), 1.78–1.88 (m, 4H), 2.16–2.40 (m, 4H), 2.88 (s, 1H), 2.96 (s, 1H), 3.53 (m, 3H), 3.72 (m, 1H), 4.24 (ddd, *J* = 8, 9.9, 2.4 Hz, 1H), 4.77 (t, *J* = 7.9 Hz, 1H), 4.85 (ddd, *J* = 7.1, 10, 2.9 Hz, 1H), 6.40 (s, 1H), 7.18 (d, *J* = 10 Hz, 1H), 7.40 ppm (d, *J* = 10 Hz, 1H); HRMS: *m/z* [M + H]⁺ calcd for C₂₃H₃₈ClN₅O₆: 516.2580, found: 516.2620. CD spectra can be found in Supporting Information figure S3.

cyclo(L-Asu(NHOH)-Aib-L-Phe-D-Pro) (**Ky-2**): This compound was synthesized according to previously reported procedures.^[13] **Ky-2** was obtained as a white powder (95 mg, 9%); *t*_R: 14.3 min (HPLC); ¹H NMR (400 MHz, CDCl₃): δ = 1.77–1.25 (m, 16H), 2.13 (m, 2H), 2.31 (m, 1H), 2.94 (m, 3H), 3.16 (m, 2H), 3.86 (m, 1H), 4.22 (d, 1H), 4.68 (d, 1H), 5.12 (m, 1H), 6.31 (d, 1H), 7.11–7.29 (m, 7H), 7.56 ppm (d, 1H); HRMS: *m/z* [M + H]⁺ calcd for C₂₆H₃₈N₅O₆: 516.2822, found: 516.2819.

General procedure for the preparation of target compounds 2a–c

cyclo(L-Am7(SAc)-Aib-L-Phe(oCl)-D-Pro) (**2a**): This compound was synthesized according to **1d** using Boc-L-Ab7 (Boc-L-α-amino-7-bromoalkanoic acid) instead of Boc-L-Asu(OBn), and Z-L-Phe(oCl)-OH instead of Z-L-Ac5-OH. After cyclization, the obtained *cyclo*(L-Ab7-Aib-L-Phe(oCl)-D-Pro) (0.8 mmol) was then dissolved in DMF (3 mL). Potassium thioacetate (1.2 mmol) was added to DMF and stirred for 4 h. After purification by silica gel chromatography and lyophilization, *cyclo*(L-Am7(SAc)-Aib-L-Phe(oCl)-D-Pro) (0.5 mmol) was obtained as a white powder (289 mg, 10%); *t*_R: 8.51 min (HPLC); mp: 70.0–70.6 °C; ¹H NMR (400 MHz, CDCl₃): δ = 1.27 (m, 2H), 1.32 (s, 3H), 1.38 (m, 2H), 1.58 (m, 2H), 1.76 (s, 3H), 1.80 (m, 2H), 1.96 (d, *J* = 8 Hz, 2H), 2.20 (m, 1H), 2.33 (s, 3H), 2.86 (t, 2H), 3.22 (m, 2H), 3.37 (m, 2H), 3.87 (m, 1H), 4.21 (m, 1H), 4.69 (d, *J* = 7 Hz, 1H), 5.34 (m, 1H), 6.11 (s, 1H), 7.11 (d, *J* = 10 Hz, 1H), 7.17 (t, 2H), 7.25 (m, 1H), 7.34 (t, 1H), 7.53 ppm (d, *J* = 10 Hz, 1H); ¹³C NMR (100 MHz, CDCl₃): δ = 23.65, 24.90, 25.02–25.41 (2C), 26.48, 28.50, 28.91–29.28 (2C), 29.40, 30.79, 33.96, 47.19, 51.70, 54.55, 57.92, 58.94, 127.04, 128.50, 129.72, 131.90, 134.47, 134.87, 172.00, 172.83, 174.56, 175.77, 196.16 ppm; ESIMS: *m/z* [M + H]⁺ calcd for C₂₇H₃₇ClN₄O₅S: 564.22, found: 565.30.

cyclo(L-Am7(SAc)-Aib-L-Phe(mCl)-D-Pro) (**2b**): This compound was synthesized according to **2a** using Z-L-Phe(mCl)-OH instead of Z-L-Phe(oCl)-OH. Compound **2b** was obtained as a white powder (285 mg, 10%); *t*_R: 8.70 min (HPLC); mp: 101.9–102.3 °C; ¹H NMR (400 MHz, CDCl₃): δ = 1.24 (m, 2H), 1.32 (s, 3H), 1.36 (m, 2H), 1.55 (m, 4H), 1.75 (s, 3H), 1.78 (m, 2H), 2.16 (m, 1H), 2.31 (s, 3H), 2.83 (t, 2H), 2.92 (m, 2H), 3.24 (m, 2H), 3.84 (m, 1H), 4.18 (m, 1H), 4.66 (d, *J* = 6 Hz, 1H), 5.11 (m, 1H), 6.11 (s, 1H), 7.10 (m, 1H), 7.18 (s, 1H), 7.21 (d, *J* = 5 Hz, 2H), 7.25 (s, 1H), 7.55 ppm (m, 1H); ¹³C NMR (100 MHz, CDCl₃): δ = 23.74, 24.92, 25.18, 26.57, 28.25, 28.51, 28.98, 29.08, 29.41, 30.82, 35.67, 47.19, 53.32, 54.52, 58.05, 59.00, 127.19, 127.44, 129.45, 130.04, 134.50, 139.25, 172.00, 172.65, 174.59,

175.88, 196.21 ppm; ESIMS: m/z $[M+H]^+$ calcd for $C_{27}H_{37}ClN_4O_5S$: 564.22, found: 565.30.

cyclo(L-Am7(SAc)-Aib-L-Phe(pCl)-D-Pro) (2c): This compound was synthesized according to **2a** using Z-L-Phe(pCl)-OH instead of Z-L-Phe(oCl)-OH. Compound **2c** was obtained as a white powder (313 mg, 10%); t_R : 8.68 min (HPLC); mp: 71.8–72.1 °C; 1H NMR (400 MHz, $CDCl_3$): δ = 1.27 (m, 2H), 1.34 (s, 3H), 1.42 (m, 2H), 1.58 (m, 4H), 1.76 (s, 3H), 2.06 (m, 2H), 2.17 (m, 1H), 2.32 (s, 3H), 2.85 (t, 2H), 2.92 (m, 2H), 3.22 (t, 2H), 3.85 (m, 1H), 4.20 (m, 1H), 4.66 (d, J = 6 Hz, 1H), 5.12 (m, 1H), 6.20 (s, 1H), 7.10 (d, J = 9 Hz, 1H), 7.17 (d, J = 7 Hz, 2H), 7.23 (t, 2H), 7.55 ppm (d, J = 9 Hz, 1H); ^{13}C NMR (100 MHz, $CDCl_3$): δ = 23.72, 24.87, 25.13, 26.48, 28.46, 28.89–29.16 (3C), 29.37, 30.79, 35.34, 47.09, 53.36, 54.48, 57.97, 58.92, 128.71–129.14 (2C), 130.45–130.74 (2C), 132.72, 135.63, 171.98, 172.70, 174.58, 175.87, 196.18 ppm; ESIMS: m/z $[M+Na]^+$ calcd for $C_{27}H_{37}ClN_4O_5S$: 564.22, found: 587.30.

Biology

Cell lines (MCF-7: human breast cancer; HeLa: human epithelial cervical cancer; K562: myelogenous leukemia, 293T: human embryonic kidney cell line) were obtained from Shanghai Institute of Biochemistry and Cell Biology (SIBS), CAS. RPMI 1640, DMEM, fetal bovine serum (FBS), and newborn calf serum (NBCS) were purchased from Gibco (USA). TSA was purchased from Sigma (USA). LipofectAmine 2000 reagent was obtained from Invitrogen (USA), pGL3-Basic plasmid was purchased from Promega (USA). BCA kit was purchased from KeyGen Biotech (China). Protein A/G plus agarose beads were obtained from Santa Cruz Biotech (USA). Anti-FLAG M2 antibody and FLAG peptide were obtained from Sigma (USA). LucLite luciferase Reporter Gene Assay Kit was purchased from Packard Instrument (USA). Antibodies anti-p21, cyclin D₁, MMP2, TIMP1, and β -actin (actin) were purchased from Santa Cruz Biotechnology (USA), and horseradish peroxidase (HRP)-conjugated affinity goat anti-mouse secondary antibodies were obtained from Invitrogen (USA). The ECL detection reagent was purchased from Thermo Scientific (USA). MTT, trypsin, and propidium iodide (PI) were purchased from Amresco (USA).

Cell culture: All cell lines were cultured under humidified air containing 5% CO₂ at 37 °C in RPMI 1640 medium supplemented with 10% NBCS (MCF-7 and HeLa cell lines) or in RPMI 1640 medium supplemented with 10% FBS (transformed mink lung epithelial cell line, MFL-9) or in DMEM supplemented with 10% FBS (K562 and 293T cell lines).

HDAC inhibitory activity: 293T cells were seeded at 2×10^6 mL⁻¹ in 100 mm dishes. After culture for 24 h, cells were transiently transfected with 10 μ g vector pcDNA3-HDAC1 for human HDAC1, pcDNA3-HDAC4 for human HDAC4, or pcDNA3-mHDA2/HDAC6 for mouse HDAC6 using LipofectAmine 2000 reagent. After successive incubation in DMEM for 24 h, the transfected cells were washed with PBS (137 mM NaCl, 2.7 mM KCl, 10 mM Na₂HPO₄, 4.2 mM KH₂PO₄, pH 7.2) and then lysed by sonication (150 W, 4 cycles of 30 s sonication, 60 s pause) in 6 mL cold lysis buffer (50 mM Tris-HCl, 120 mM NaCl, 5 mM EDTA, and 0.5% NP-40, pH 7.5). The soluble fraction was pre-cleared by incubation with protein A/G plus agarose beads. After collection by microcentrifugation (12000 rpm, 12800 g) for 2 min at 4 °C, the pre-cleared supernatant was then incubated with 4 μ g anti-FLAG M2 antibody probing for HDAC1, HDAC4, or HDAC6 for 1 h at 4 °C. The agarose beads were washed three times with lysis buffer and once with histone deacetylase restore buffer (20 mM Tris-HCl, 150 mM NaCl, and 10% glycerol, pH 8.0). The obtained immune complex was then in-

cubated with 40 μ g FLAG peptide in restore buffer (200 μ L) for 1 h at 4 °C to release HDACs. The supernatant was collected by centrifugation (12000 rpm, 12800 g) for 10 min at 4 °C. For inhibitory activity assays against HDACs, 10 μ L enzyme fraction was added into the mixture composed of 1 μ L fluorescent substrate (2 mM Ac-KGLGK (Ac)-MCA) and 9 μ L restore buffer. After incubation at 37 °C for 30 min, 30 μ L trypsin solution (20 mg mL⁻¹) was added to the reaction mixture and incubated at 37 °C for 15 min to stop the reaction. The released product, aminomethyl coumarin (AMC), was measured using a fluorescence plate reader (Thermo Varioskan Flash, USA) at λ 252 nm.

p21 promoter assay: This assay was performed as described previously using a stably transformed cell line, namely MFL-9.^[31] MFL-9 expresses a low level of luciferase, the activity of which can be enhanced by TSA in a dose-dependent manner. MFL-9 cells (1×10^5) were cultured in a 96-well plate for 6 h and then incubated for 18 h under identical conditions in the absence or presence of desired concentrations of test compounds. After treatment, cells were collected and lysed in the manner as mentioned above. The luciferase activity of each cell lysate was measured with a LucLite luciferase reporter gene assay kit and recorded using a Luminescencer-JNR luminometer (ATTO, Tokyo, Japan). All data were normalized to the protein concentration of cell lysate before they were used for analysis. Concentrations at which a compound induces the luciferase activity 10-fold higher than the basal level are presented as the 1000% effective concentration (EC₁₀₀₀).

MTT assay: Cells in logarithmic growth phase were equally seeded in a 96-well plate at a density of 1×10^4 cells per well. Cells were cultured in complete growth medium for 24 h and then exposed to various concentrations of test compounds. Cells used as negative control were exposed to DMSO under the same conditions. After the 48 h incubation, 20 μ L MTT solution (5.0×10^3 mg L⁻¹ diluted in PBS) was added to each well. For solid tumor cells (MCF-7 and HeLa cells), after incubation with MTT for 3 h, formazan formed from MTT was dissolved in 200 μ L DMSO and mixed for 10 min before measurement. For K562 cells, lysis solution (50% DMF (v/v), 30% SDS (w/v)) was added to dissolve formazan. The optical density was measured with an ELISA reader (Sunrise, Japan) at 570/630 nm. The percent inhibition was calculated as per Equation (1):

$$\% \text{ inhib.} = [1 - (A_{570 \text{ sample}} - A_{630 \text{ sample}}) / (A_{570 \text{ ctrl}} - A_{630 \text{ ctrl}})] \times 100 \quad (1)$$

Flow cytometry analysis: MCF-7 cells were seeded at 2×10^5 mL⁻¹ in six-well plated. The adherent cells were treated with increasing concentrations of compound **1b** ranging from 6.5 to 26 nM. After 24 h incubation, cells were detached using trypsin and then harvested by centrifugation for 5 min at 2000 rpm (360 g). Cells (1×10^5) were then separated for detection. After washing twice with cold PBS (4 °C), the cell pellets were fixed in 75% EtOH at -20 °C overnight. The pellets were washed twice with cold PBS, and then suspended in 200 μ L PI solution (50 mg L⁻¹ PI, 1% (v/v) Triton X-100 in PBS). After incubation at 4 °C for 20 min in the dark, cells were measured using a BD FACSCanto flow cytometer (USA), and the results were analyzed using Mod Fix LT 3.0 software.

Western blots: After treatment, cells were harvested, washed with cold PBS, and then lysed in lysis buffer (50 mM Tris-HCl, 1% Triton X-100, 10% glycerol, 1 mM PMSF, 1 mM DTT, 20 μ g mL⁻¹ aprotinin, pH 6.8) at 0 °C for 1 h. The lysates were clarified by centrifugation (15000 rpm, 20000 g) for 10 min at 4 °C. Total protein concentration of the soluble cell extract was determined using a BCA kit before electrophoresis. Same amount of protein was run on

a 12.5% (for cyclin D₁, MMP2, TIMP1, and β -actin) or 15% (for p21 and β -actin) SDS-PAGE gel and then electrophoretically transferred onto a PVDF membrane. The membrane was subsequently blocked with 5% (w/v) non-fat milk in TBST saline (20 mM Tris-HCl, 150 mM NaCl, 0.05% (v/v) Tween-20) overnight at 4 °C. The blocked membrane was then incubated successively with primary antibody (diluted 1:800–1:1000) at 4 °C overnight, then HRP-labeled goat anti-mouse secondary antibody (diluted 1:2000) at 37 °C for 1 h. After incubation, the membrane was washed with TBST and the immunoreactive bands were visualized using an ECL reagent kit according to the manufacturer's instructions.

Soft agar assay: For soft agar assay, cells were diluted to the desired concentration (300 per well) in the upper agar layer (0.03% agar in normal medium) in the absence or presence of compound **1b** after the lower layer (2.0% agar in drug-free normal medium) was plated as previously described.^[32] After successive incubation for 10–14 days, when colonies were large enough for visualization by microscopy (Olympus, 1X71), MTT (200 μ L) was added to each well for visualization.

Gelatin zymography: This assay was performed as described previously.^[42] Generally, MCF-7 cells were seeded into six-well plate and maintained for 24 h for adherence. The cells were then treated with compound **1b** in serum-free medium for various times. After treatment, the conditioned medium was collected, mixed with loading buffer, and then electrophoresed on a 10% SDS-PAGE gel containing 0.1% (w/v) gelatin. After electrophoresis, the gel was washed two times in refolding buffer (50 mM Tris-HCl, 200 mM NaCl, 10 mM CaCl₂, 2.5% (v/v) Triton X-100, pH 7.4) to remove SDS. Then the refolded gel was soaked in reaction buffer (50 mM Tris-HCl, 200 mM NaCl, 10 mM CaCl₂, 0.02% Brij-35, pH 7.4) at 37 °C for 36 h. After reaction, the gel was stained for 3 h with staining solution (0.1% Coomassie Brilliant Blue, 30% MeOH, and 10% AcOH), and then destained in destaining solution (30% MeOH and 10% AcOH in distilled H₂O) until clear bands against the dark-blue background could be visualized.

Docking: Docking studies were conducted with AutoDock 4.2 using Lamarckian genetic algorithm.^[43] Initial structures of HDAC2 and HDAC4 were modeled from the atom coordinates of the X-ray crystal structure (PDB IDs: 3MAX for HDAC2, 2VQJ for HDAC4).^[44,45] Target compound was located near the active site of HDAC. A grid size of 70 \times 70 \times 70 points with a spacing of 0.375 Å between the grid points was implemented to cover the entire surface of HDAC. For the tested compounds, all single bonds except the amide bonds and cyclic bonds were treated as active torsional bonds; 150 independent dockings (150 runs) were performed using genetic algorithm searches. A maximum number of 2.5 \times 10⁶ energy evaluations and a maximum number of 5000 generations were implemented during each genetic algorithm run. A mutation rate of 0.02 and a crossover rate of 0.8 were used. Other parameters were all set as default in AutoDock 4.2. The PyMOL (<http://www.pymol.org>) and LigPlot programs were also used to analyze the docking results, focusing on hydrogen bonds and hydrophobic interactions.^[46] Hydrogen bonds with a donor–acceptor distance < 3.5 Å were represented.

Statistics: All data represented at least three independent experiments and are expressed as the mean \pm SD unless otherwise indicated. Statistical comparisons were made by Student *t*-test and one-way ANOVA method using Origin 8.0.

Acknowledgements

We acknowledge Dr. Alan Chang for his help in the revision of this manuscript.

Keywords: cell migration • chlamydocin analogues • cyclic tetrapeptides • docking • HDAC inhibitors

- [1] N. Sengupta, E. Seto, *J. Cell. Biochem.* **2004**, *93*, 57–67.
- [2] J. S. Lee, E. Smith, A. Shilatifard, *Cell* **2010**, *142*, 682–685.
- [3] W. S. Xu, R. B. Parmigiani, P. A. Marks, *Oncogene* **2007**, *26*, 5541–5552.
- [4] M. Yoshida, M. Kijima, M. Akita, T. Beppu, *J. Biol. Chem.* **1990**, *265*, 17174–17179.
- [5] C. Choudhary, C. Kumar, F. Gnad, M. L. Nielsen, M. Rehman, T. C. Walther, J. V. Olsen, M. Mann, *Science* **2009**, *325*, 834–840.
- [6] S. Kim, R. Sprung, Y. Chen, Y. Xu, H. Ball, J. Pei, T. Cheng, Y. Kho, H. Xiao, L. Xiao, N. V. Grishin, M. White, X. Yang, Y. Zhao, *Mol. Cell* **2006**, *23*, 607–618.
- [7] M. Dokmanovic, C. Clarke, P. A. Marks, *Mol. Cancer Res.* **2007**, *5*, 981–989.
- [8] A. Valenzuela-Fernández, J. R. Cabrero, J. M. Serrador, F. Sanchez-Madrid, *Trends Cell Biol.* **2008**, *18*, 291–297.
- [9] M. Y. Ahn, D. O. Kang, Y. J. Na, S. Yoon, W. S. Choi, K. W. Kang, H. Y. Chung, J. H. Jung, D. S. Min, H. S. Kim, *Cancer Lett.* **2012**, *325*, 189–199.
- [10] N. A. P. Franken, H. M. Rodermond, J. Stap, J. Haveman, C. V. Bree, *Nat. Protoc.* **2006**, *1*, 2315–2319.
- [11] J. Tan, S. Cang, Y. Ma, R. L. Petrillo, D. Liu, J. Hematol, *Oncology* **2010**, *3*, 5.
- [12] A. A. Lane, B. A. Chabner, *J. Clin. Oncol.* **2009**, *27*, 5459–5468.
- [13] S. Fujii, T. Okinaga, W. Ariyoshi, O. Takahashi, K. Iwanaga, N. Nishino, K. Tomimaga, T. Nishihara, *Biochem. Biophys. Res. Commun.* **2013**, *434*, 413–420.
- [14] N. Nishino, B. Jose, R. Shinta, T. Kato, Y. Komatsu, M. Yoshida, *Bioorg. Med. Chem.* **2004**, *12*, 5777–5784.
- [15] A. P. Kozikowski, K. V. Butler, *Curr. Pharm. Des.* **2008**, *14*, 505–528.
- [16] A. De Ruijter, A. H. Van Gennip, H. N. Caron, S. Kemp, A. Van Kuilenburg, *Biochem. J.* **2003**, *370*, 737–749.
- [17] C. J. Millard, P. J. Watson, I. Celardo, Y. Gordiyenko, S. M. Cowley, C. V. Rpbinson, L. Fairall, J. W. R. Schwabe, *Mol. Cell* **2013**, *51*, 57–67.
- [18] G. M. Shivashimpi, S. Amagai, T. Kato, N. Nishino, S. Maeda, T. G. Nishino, M. Yoshida, *Bioorg. Med. Chem.* **2007**, *15*, 7830–7839.
- [19] D. Huang, X. Li, L. Sun, Z. Xiu, N. Nishino, *J. Pept. Sci.* **2012**, *18*, 242–251.
- [20] W. Gu, I. Nusinzon, R. D. Smith, C. M. Horvath, R. B. Silverman, *Bioorg. Med. Chem.* **2006**, *14*, 3320–3329.
- [21] T. A. Miller, D. J. Witter, S. Belvedere, *J. Med. Chem.* **2003**, *46*, 5097–5116.
- [22] K. B. Glaser, *Biochem. Pharmacol.* **2007**, *74*, 659–671.
- [23] S. Schäfer, L. Sauders, E. Eliseeva, A. Velena, M. Jung, A. Schwienhorst, A. Strasser, A. Dickmanns, R. Ficner, S. Schlimme, W. Sippl, E. Verdin, M. Jung, *Bioorg. Med. Chem.* **2008**, *16*, 2011–2033.
- [24] Y. Chen, M. Lopez-Sanchez, D. N. Savory, D. D. Billadeau, G. S. Dow, A. P. Kozikowski, *J. Med. Chem.* **2008**, *51*, 3437–3448.
- [25] E. S. Inks, B. J. Josey, S. R. Jesinkey, C. J. Chou, *ACS Chem. Biol.* **2012**, *7*, 331–339.
- [26] T. Suzuki, A. Kouketsu, Y. Itoh, S. Hisakawa, S. Maeda, M. Yoshida, H. No-kagawa, N. Miyata, *J. Med. Chem.* **2006**, *49*, 4809–4812.
- [27] C. Florean, M. Schneckbyrger, C. Grandjenette, M. Diederich, *Epigenomics* **2011**, *3*, 581–609.
- [28] C. Bradbury, F. Khanim, R. Hayden, C. Bunce, D. White, M. Drayson, C. Craddock, B. Turner, *Leukemia* **2005**, *19*, 1751–1759.
- [29] K. Harada, G. R. Ogdan, *Oral Oncol.* **2000**, *36*, 3–7.
- [30] D. Dubravka, D. W. Scott, *Cell Res.* **2000**, *10*, 1–16.
- [31] R. Debret, S. Brassart-Pasco, J. Lorin, A. Martoriati, A. Deshorgue, F. Maquart, I. Rahman, F. Antonicelli, *Biochim. Biophys. Acta Mol. Cell Res.* **2008**, *1783*, 1718–1727.
- [32] K. Kessenbrock, V. Plaks, Z. Werb, *Cell* **2010**, *141*, 52–67.

- [33] L. M. Coussens, B. Fingleton, L. M. Matrisian, *Science* **2002**, *295*, 2387–2392.
- [34] E. Y. Lin, A. V. Nguyen, R. G. Russell, J. W. Pollard, *J. Exp. Med.* **2001**, *193*, 727–739.
- [35] R. Brunmeir, S. Lagger, C. Seiser, *Int. J. Dev. Biol.* **2009**, *53*, 275–289.
- [36] H. Jeon, L. T. Zheng, S. Lee, W. H. Lee, N. Park, J. Y. Park, W. D. Heo, M. S. Lee, K. Suk, *Exp. Cell Res.* **2011**, *317*, 2007–2018.
- [37] V. Duong, C. Bret, L. Altucci, A. Mai, C. Duraffourd, J. Loubersac, P. Harmand, S. Bonnet, S. Valente, T. Maudelonde, V. Cavailles, N. Boulle, *Mol. Cancer Res.* **2008**, *6*, 1908–1919.
- [38] B. Bardeda-Zahonero, M. Parra, *Mol. Oncol.* **2012**, *6*, 579–589.
- [39] I. M. Clark, T. E. Swingler, C. L. Sampieri, D. R. Edwards, *Int. J. Biochem. Cell Biol.* **2008**, *40*, 1362–1378.
- [40] A. Suminoe, A. Matsuzaki, H. Hattori, Y. Koga, E. Ishii, T. Hara, *Leukemia Res.* **2007**, *31*, 1437–1440.
- [41] E. A. Stronach, A. Alfraid, N. Rama, C. Dalter, J. B. Studd, R. Agarwal, T. G. Guney, C. Gourley, B. T. Hennessy, G. B. Mills, A. Mai, R. Brown, R. Dina, H. Gabra, *Cancer Res.* **2011**, *71*, 4412–4422.
- [42] P. A. M. Snoek-van Beurden, J. W. Von den Hoff, *BioTechniques* **2005**, *38*, 73–83.
- [43] G. M. Morris, D. S. Goodsell, R. S. Halliday, R. Heuy, W. E. Hart, R. K. Belew, A. J. Olson, *J. Comput. Chem.* **1998**, *19*, 1639–1662.
- [44] J. C. Bressi, A. J. Jennings, R. Skene, Y. Wu, R. Melkus, R. D. Jong, S. O'Connell, C. E. Grimshaw, M. Navre, A. R. Gangloff, *Bioorg. Med. Chem. Lett.* **2010**, *20*, 3142–3145.
- [45] M. J. Bottomley, P. L. Surdo, P. D. Giovine, A. Cirillo, R. Scarpelli, F. Ferrigno, P. Jones, P. Neddermann, R. D. Francesco, C. Steinkuhler, P. Gallinari, A. Carfi, *J. Biol. Chem.* **2008**, *283*, 26694–26704.
- [46] A. C. Wallace, R. A. Laskowski, J. M. Thornton, *Protein Eng.* **1995**, *8*, 127–134.

Received: September 15, 2013

Revised: November 6, 2013

Published online on November 27, 2013